Chapter 1

# A Fractal Model of the Stress Field Around a Rough Crack

Lucas Máximo Alves, Marcio Ferreira Hupalo,
Selauco Vurobi Júnior and Luiz Alkimin de Lacerda

Additional information is available at the end of the chapter

http://dx.doi.org/10.5772/64998

**Abstract**

This chapter presents a model of a stress and displacement fields around a rough crack tip in brittle and ductile materials using a pre-fractal model. This approach allows for a more realistic fractal scaling, of a real fracture. A special stress vector for rugged surfaces was defined, and it was also shown that the pre-fractal consideration also results in different asymptotic limits for the singularity degree of the stress field at the crack tip for brittle materials. The asymptotic limit obtained here differs from the singularity degrees presented by other authors. Therefore, other consequences such as fracture instability are also included in the mathematical model presented here. A generalization of the stress fields for brittle and ductile materials is proposed. Changes in geometric shapes of the stress field are due to the roughness at the crack tip as shown by the mapping of simulated stress fields around a crack tip. The fractal stress field functions were mapped at different singularity power degrees indicating that the qualitative aspects of these fields alone, do not sufficient to determine which model presents the best fit to experimental results. Therefore, the model need a validation based on quantitative experimental measurements.

**Keywords:** stress field, fractal fracture mechanics, fractal dimension, Hurst dimension, stress intensity factor

## 1. Introduction

In classical fracture mechanics theory, a brittle material has an asymptotic stress field, whose singularity exponent depends on the distance from the crack tip, which Hutchinson [1] define as :

$$\sigma_{I,II,III}(r) \sim \frac{K_{I,II,III}}{r^{n/n+1}} \left(p/n=1\right) \tag{1}$$

where $n = 1$ is the degree of homogeneity of the distribution of the elastic stress field given by Hooke's Law. This singularity is part of discussion in the literature on rough fractal cracks are considered.

Mosolov [2–4] attempted to explain crack growth under compression based on the fractality of cracks. He was the first researcher to study and theorize about changes in the stress field singularity magnitude according to the fractality of rough crack surfaces in mesoscale dimensions. He showed that the stress at the crack tip of a fractal crack under uniform compressive stress is unique. Mosolov [2–6] stated that the singularity in the stress field in front of a rough fractal crack should be corrected by means of a fractional exponent. He also suggested that the elastic field ahead of the crack tip should have a fractional singularity exponent associated to the asymptotic dependence on the distance, represented by [2–4]:

$$\sigma_{I,II,III}(r) \sim \frac{K_{I,II,III}}{r^{n/n+1}} \left(p/n \neq 1\right) \rightarrow \sigma_{I,II,III}(r) \sim \frac{K_{I,II,III}}{r^{\alpha}} \tag{2}$$

This is because the stress field is primarily responsible by generate the noise of a crack or fracture surface in a solid body subjected to the action of a strain loading which is transferred for the formation of new surfaces through of an elastic or elastic-plastic energy releasing rate in the fracture phenomenon, as follows:

$$\sigma(r) \rightarrow G(L) \rightarrow 2\gamma_{eff} \tag{3}$$

After Mosolov's observation [2–6], Borodich [7–8] began to develop a fracture criterion involving the roughness of a crack based on fractal theory. These two authors established the mathematical relationships between the elastic stress field around a crack or fracture surface and the fractal roughness exponent of a fracture surface, using the dependence of the fractional exponents of singularity of the field at the crack tip and the fractional dependence of the fractal exponents of the scaling of fracture surfaces. Using the Griffith criterion, and considering the fact that the actual length of a fractal crack is larger than its apparent size, they came up with the asymptotic expression for a self-similar fractal crack in Mode I. They did this by comparing the stress field, as shown in the following equation:

$$\Delta U_L(L) \sim r^{-2\alpha} L^2 = \Delta U_\gamma \sim 2\gamma_{eff} L^D \tag{4}$$

Where $D$ is the so-called Hausdorff-Besicovitch fractal dimension [9, 10] of a self-similar crack. Note that there are many definitions for the fractal dimension. All these definitions give the same fractal dimension for a self-similar fractal.

Cherepanov and Balankin [11–13] attempted to define a relationship between the exponent $\alpha$ suggested by Mosolov [2–4] and the fractal topology of a rough crack. Later, Balankin [12, 13] published a series of papers proposing a complete modification of fracture mechanics, from linear elasticity theory to nonlinear elastic fracture mechanics. Based on a dimensional analysis such as that shown in (4), Balankin [13] found in self-affine fractal cracks the same degree of singularity of the stress field as that proposed by Mosolov for a self-similar fractal crack. The relationship proposed by Balankin [12, 13] was as follows:

$$\sigma_{I,II,III}(r) \sim \frac{K_{I,II,III}}{r^{\alpha}} \quad p/\alpha = \begin{cases} \dfrac{2-D_B}{2} = \dfrac{H}{2} & p/d = 1 \\ \dfrac{3-D_B}{2} = \dfrac{H}{2} & p/d = 2 \end{cases} \tag{5}$$

where $D_B$ is the so-called Hausdorff-Besicovitch [9, 10] fractal box dimension for a self-similar crack. Thus, Mosolov and Balankin established mathematical relationships between the elastic stress field around the crack and the roughness parameter of the fracture surface. It should be noted that Eq. (5) results in $\alpha = H/2$ in the two aforementioned cases. The consequences of this mathematical result for fracture mechanics could not be fully confirmed through experimental results. On the other hand, it was also not possible to establish a relationship between the model Mosolov [2, 3]and the other fundamental consequences he proposed for fractures.

Realizing the limitations of the Mosolov model [2, 3], Balankin [12, 13] and Yavari [14–16] proposed a new approach to stress field singularity exponents and developed his model to its ultimate consequences. He even proposed two new fracture modes and a discrete fracture mechanics that combined the fractal theory with quantum aspects of the fracture described by Pugno and Ruoff [17]. Yavari [14–16] also discussed the earlier expressions proposed by Mosolov [7] in (2), as well as the model proposed by Balankin [12]. However, unlike Mosolov [2, 3], he found a relationship between the singularity exponent using (4) and substituted the box-dimension $D_B$ by the divider dimension, $D_D = d/H$. He argued that the stress field at the fractal crack tip should satisfy the following expression:

$$\sigma(r) \sim \frac{K_{I,II,III}}{r^{\beta}} \quad p/\beta = \begin{cases} \dfrac{2-D_D}{2} = \dfrac{2H-1}{2H} & p/d = 1 \\ \dfrac{3-D_D}{2} = \dfrac{3H-2}{2H} & p/d = 2 \end{cases} \tag{6}$$

Yavari [14, 15] then proposed a systematic approach for calculating the magnitude of stress field and singularity degree for fractal cracks, using the force lines method, which is applicable

to all fracture modes. He considered the three classical fracture modes for fractal cracks and made a more in-depth investigation of the problem of stress singularity at the crack tip. Alternatively, however, this chapter proposes a new approach to the problem of stress field singularity, considering a geometrical instability coefficient, $\beta_L$, to correct the Cauchy stress field around a crack, which is defined in Euclidean geometry, and changing for a fractal stress field, in the following way:

$$\sigma = \frac{\sigma_0}{\beta_L} \tag{7}$$

where the new singularity exponent $\alpha$ for the stress field is:

$$\sigma_{I,II,III}(r) \sim \frac{K_{I,II,III}}{r^{\alpha}} \quad p/\alpha = \frac{3-2H}{2} \quad p/d = 1,2 \tag{8}$$

Eqs. (7) and (8) are consistent with the experimental measurements and mathematical developments made to date [18–25]. These mathematical results are considered the most acceptable and realistic corrections and are therefore adopted and developed throughout this chapter. The proposal presented here is based on the relationship between the rough crack length and its Euclidean projection, which is given by Alves [18–25], i.e., the rough crack length was considered as $L \sim l_0 n^{1-H}$, where $l_0$ is the minimum permissible size for the advance of a crack. Therefore, it was also considered that the box dimension, $D_B$ is able to portray the irregularities associated with microregions of strain around a two-dimensional (2D) crack and the three-dimensional (3D) fracture surface. In terms of the crack length or area of the fracture surface, our proposal differs from that of Yavari [14–16], who considered that the rough crack length is of the type: $L \sim l_0 n^{\frac{1}{H}}$, using the divider dimension $D_D$, which represents only the irregularities on the noisy line of the crack or on the fracture surface, without considering the effects of strain in the microregions around the crack.

## 2. Theoretical development: analysis of the influence of the crack roughness on the stress field at the crack tip

The use of fractal measure theory to model fracture phenomena is of great interest in the mathematical development of Fractal Fracture Mechanics. The roughness of a real crack extends within a finite limit ranging from a lower to an upper fractal cut-off scale. However, the fractal models for fracture proposed by several authors presuppose a fractal crack with an infinite range of self-affine scales that cannot be verified experimentally. It is known that a real crack has limits imposed by a finite number of fractal scales ranging from a lower fractal cut-

off scale to an upper fractal cut-off scale. In a real fracture, the finite limits of fractal scales are always compatible with the minimum microcrack and with the length of the macroscopic crack in the sample. Thus, the lower fractal cut-off scale is given by the characteristic size of a microcrack, while the length of the macroscopic crack on the specimen indicates the upper fractal cut-off scale. Therefore, fractal models of fracture phenomena require a more realistic approach that takes into account the limits of scales and singularity exponents, and hence, the fractal scales that are actually found in a real fracture.

To model the real movement of the crack tip, one must consider a infinitesimal element of length of a rough crack with its corresponding flat Euclidean projection, as shown in Figure. Thus, all the quantities previously considered and associated with the projected length of a crack must be rewritten in terms of the actual rough crack length. Hence, the stress field will be modified by some function of the type:

$$\sigma = \sigma_0 f\left(L/L_0\right) \tag{9}$$

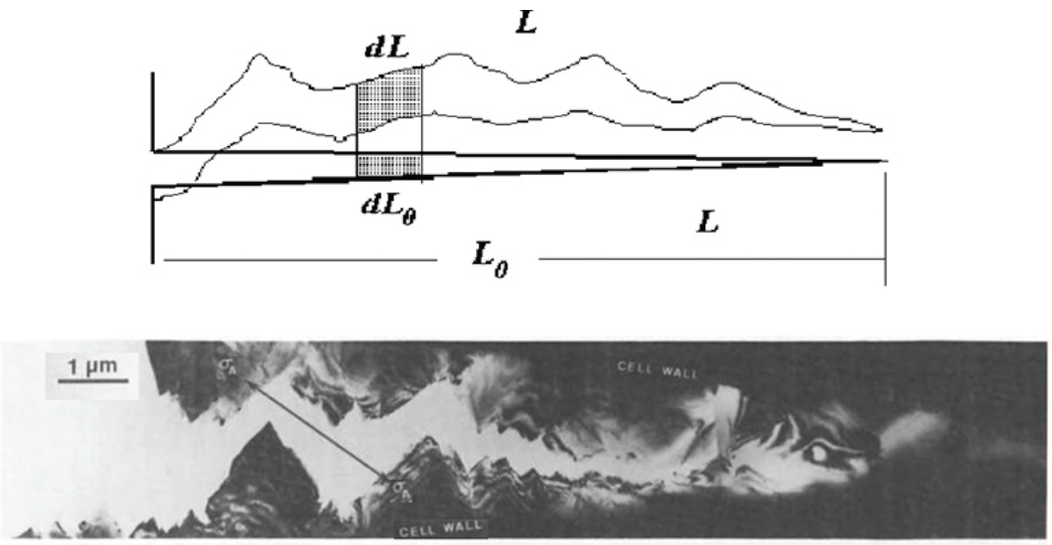


**Figure 1.** Rough crack with an energy-equivalent flat projection. Figure adapted from Ohr [26].

Consequently, all the other quantities of the fracture mechanics will also be modified analogously. As can be seen in **Figure 1**, a crack grows with variations in the coordinates of its tip that follow a rough path, having both a microscopic and a macroscopic velocity, which produce the surface roughness and its macroscopic path, respectively.

**Figure 2** presents experimental results obtained by Ohr in 1985 [26]. These results demonstrated experimentally that the aspect of the stress field in front of a crack appears deformed because of its roughness. Also, according to Xin [27], inclined crack models show that the appearance of the stress field ahead of the crack tip is distorted relative to a non-inclined crack. This supports the proposal of this chapter that roughness affects both the intensity of the field as its geometric aspect.

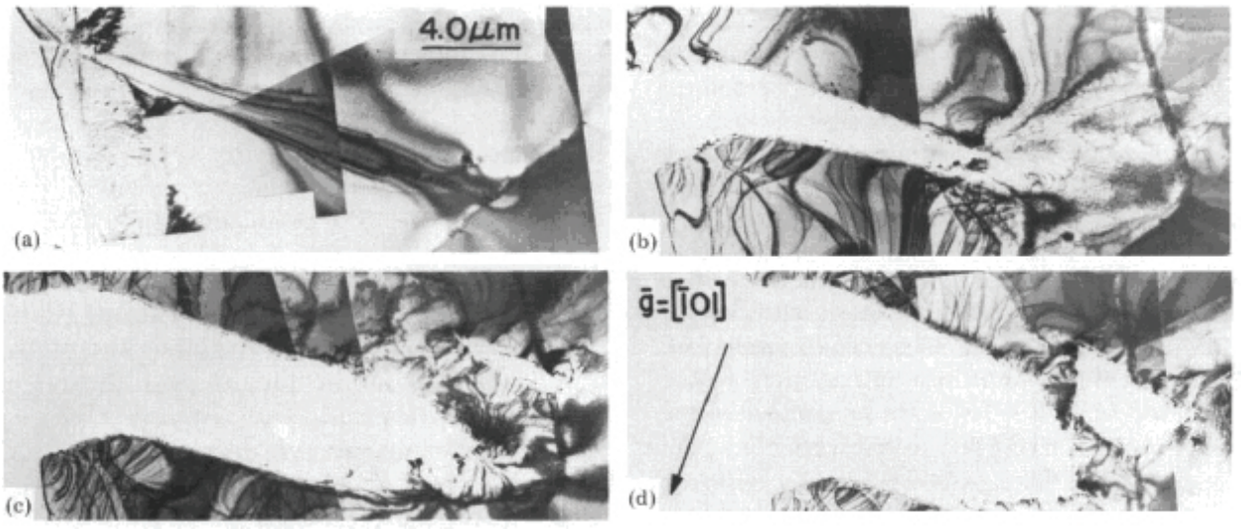


**Figure 2.** Influences of surface roughness of a crack and the appearance of the stress field at its tip, shown by a series of electron micrographs depicting the interaction between a crack and a grain boundary in molybdenum. As the crack approaches the boundary, a small crack is nucleated and eventually joined the main crack. Figure adapted with permission from Ohr [26].

The geometric instability coefficient of a crack with a fractal roughness, which is given in (7), can be generalized based on the following arguments: (i) experimental observations; (ii) previous arguments about the influence of roughness on intensity; (iii) geometric aspect of the stress field at the crack tip; and (iv) the coherent mathematical development; and a correction can be proposed for the mathematical solution of the rough stress field, using a quantity $\beta_L$. This quantity, which gives the ratio between rough and smooth lengths for global influence, multiplied by the ratio of their infinitesimal differences for local influence, can be called the *geometric instability coefficient of the crack*, as follows:

$$\beta_L = \underbrace{\frac{L}{L_0}}_{global}\underbrace{\frac{dL}{dL_0}}_{local} \tag{10}$$

This coefficient reflects the interaction between the local and global aspects of the crack length.

Considering a self-affine fractal crack, according to Alves et al. [18, 22, 23], the coefficient of geometric instability, which depends on the roughness at the crack tip, is given as follows:

$$\beta_L\left(H, l_0, L_0\right) \equiv \frac{L}{L_0}\frac{dL}{dL_0} = \frac{1}{2}\left[1 + \left(2 - H\right)\left(\frac{l_0}{L_0}\right)^{2H-2}\right] \tag{11}$$

Since there is a relationship between the distance $r$ in front of the crack and the fractality at its tip in the region of the concentrated stress field, the quantities $r$ and rough length $L$ are closely

http://dx.doi.org/10.5772/64998

related, following the "principle of equivalence of the closed crack". Hence, it is possible that the stress field intensities, $\sigma$ begins to depend on both $r$ and $L$ to the point that a single dependency arises between these quantities, as shown by Yavari [14, 15]. However, this is only possible if the asymptotic limits of the crack proposed by Yavari [14, 15] actually occur in a real crack; otherwise, a simple roughness behaves exactly like a local field strength modifier and not like a change in the degree of singularity.

In regions near the crack tip $(L, L_0 \sim r(x,y) \to 0)$ the term $(2-H)\left(l_0/L_0\right)^{2H-2} >> 1$, hence, Eq. (11) can be written as:

$$\beta_L\left(H, l_0, L_0\right) \equiv \frac{L}{L_0}\frac{dL}{dL_0} = \left(2-H\right)\left(\frac{l_0}{L_0}\right)^{2H-2} \tag{12}$$

The geometric instability coefficient of a crack in its complex form can be defined as:

$$\beta_L\left(z, H\right) = \left(2-H\right)\left(\frac{l_0}{z}\right)^{2H-2} \tag{13}$$

where the Cartesian coordinates $x$ and $y$ originate at the crack tip. The coefficient of instability of the fracture surface in its polar form, $z = re^{i\theta}$ can also be written as:

$$\beta_L\left(H, r, \theta\right) = \left(2-H\right)\left(\frac{l_0}{r}\right)^{2H-2}\left(\cos\left[\left(2-2H\right)\theta\right] + i\,\mathrm{sen}\left[\left(2-2H\right)\theta\right]\right) \tag{14}$$

Therefore, one can propose that the complex function of Westergaard, $Z$ [28], which depends on $z = x + iy$, should be modified by adding the coefficient of instability of the fracture surface given in (10) as:

$$\beta_L^{1/2}\left(z, H\right) = \sqrt{\left(2-H\right)}\left(\frac{l_0}{z}\right)^{\frac{2H-2}{2}} \tag{15}$$

Its polar form $z = re^{i\theta}$ is considered as:

$$\beta_L^{1/2}\left(H, r, \theta\right) = \sqrt{\left(2-H\right)}\left(\frac{l_0}{r}\right)^{\frac{2H-2}{2}}\left(\cos\left[\frac{\left(2-2H\right)}{2}\theta\right] + i\,\mathrm{sen}\left[\frac{\left(2-2H\right)}{2}\theta\right]\right) \tag{16}$$

The graphic of ${\beta_L}^{1/2}$ as a function of $x + iy$ is shown in **Figure 3**. In this figure, note that there is a forbidden area with a value of $r \leq l_0$ and $r \geq L_0$, and also an oscillation angle of the crack, $\theta_{\min} \leq \theta \leq \theta_{\max}$, which varies according to the value of the Hurst exponent $H$. For the value $H = 1.0$ that corresponds to a smooth crack, the oscillation angles are zero, $\theta_{\min} = \theta = \theta_{\max} = 0$, because there is no angle variation in a smooth crack. This is in line with the intuitive idea that a crack generally oscillates around the direction of propagation. The results shown in **Figure 3** confirm a previous mathematical finding that a rough crack has limit angles of propagation for opening of its angular oscillations [25]. Now, in this chapter, these limit angles have been related with the Hurst exponent of crack roughness, where the entropy for a rough line is given by:

$$\langle S \rangle = -k\left(\frac{h_0}{H_0 \cos(\varsigma\pi)}\right)\ln\left(\frac{h_0 l_0}{H_0 L_0 \cos(\varsigma\pi)}\right) \tag{17}$$

for $-\varsigma\pi \leq \theta \leq \varsigma\pi$, where $\varsigma = 1 - H$. The complex coefficient of instability, ${\beta_L}^{1/2}$ of the fractal stress field, shows that this stress field will be affected in its degree of singularity and in its intensity as will be shown by the conformal mapping across the plane stress around the crack.

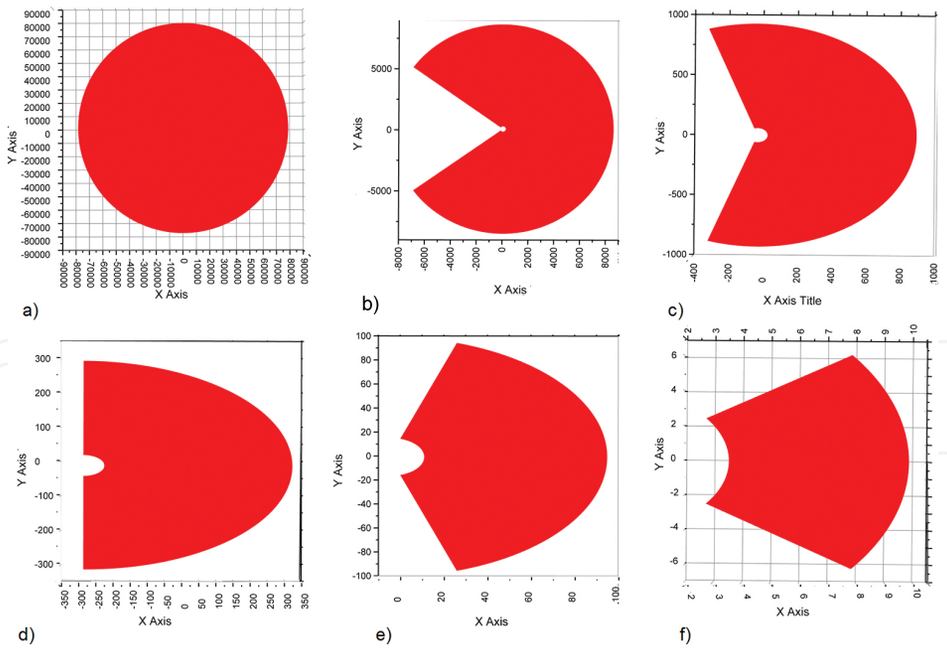


**Figure 3.** Complex map of the variation in fractal roughness of the crack given by Eq. (16) for: a) $H = 0.0$ with $-\pi \leq \theta \leq \pi$; (b) $H = 0.2$ with $-0.8\pi \leq \theta \leq 0.8\pi$; (c) $H = 0.4$ with $-0.6\pi \leq \theta \leq 0.6\pi$; (d) $H = 0.5$ with $-0.75\pi \leq \theta \leq 0.75\pi$; (e) $H = 0.6$ with $-0.4\pi \leq \theta \leq 0.4\pi$; (f) $H = 0,8$ with $-0.2\pi \leq \theta \leq 0.2\pi$ and $l_0 = 0,001$, for the interval of $-50 \leq r \leq 50$.

http://dx.doi.org/10.5772/64998

## 3. Modeling the fractal stress field around a rough crack

There are three independent movements that correspond to the three fundamental fracture modes, as pointed out by Irwin [29]. These basic fracture modes are usually called Mode I, Mode II, and Mode III, respectively, and any fracture mode in a cracked body may be described by one of the three basic modes, or by combinations thereof.

The Airy-Westergaard function for the stress field with fractal roughness can be determined based on the foregoing arguments about the influence of roughness on the intensity and the geometrical aspect of the stress field at the crack tip. Based on the mathematical development performed here, we propose that the Westergaard complex function, $\phi$ which depends on $z = x + iy$ should be modified by adding the parameter ${\beta_L}^{1/2} = \sqrt{\left(L/L_0\right)dL/dL_0}$ as follows:

$$\phi_{I,II,III}\left(z,\beta_L\left(z,H\right)\right) = \frac{K_{I,II,III}}{\left(2\pi z\beta_L\left(z,H\right)\right)^{1/2}} \tag{18}$$

where the three parameters $K_I, K_{II}$ and $K_{III}$ are called stress intensity factors that correspond to the opening, sliding, and tearing (anti-plane shearing) fracture modes, respectively. These expressions indicate that the stresses have an inverse square root singularity at the crack tip and that the stress intensity factors $K_I, K_{II}$ and $K_{III}$ measure the intensities of the singular stress fields of opening, in-plane shearing, and anti-plane shearing, respectively. The stress intensity factor, a new concept in solids mechanics, plays an essential role in the study of the fracture strength of cracked solids. Substituting (15) in (18), one has:

$$\phi_{I,II,III}\left(H,z\right) = \frac{K_{I,II,III}}{\left[2\pi z\left(2-H\right)\left(\frac{l_0}{z}\right)^{2H-2}\right]^{\frac{1}{2}}} \tag{19}$$

and grouping similar terms, one has:

$$\phi_{I,II,III}\left(H,z\right) = \frac{K_{I,II,III}}{\sqrt{2\pi\left(2-H\right)l_0}}\left(\frac{l_0}{z}\right)^{\frac{3-2H}{2}} \tag{20}$$

Considering the above conditions, we propose the following stress function due to the dominant term of the stress function around the tip of a fractal crack. Therefore, the potential function $\phi$ depends on $z = x + iy$ and the fractal exponent of the crack is $\alpha = (3-2H)/2$. By replacing the complex variable $z$ for its polar form, according to Euler, $z = re^{i\theta}$ where $r$ and $\theta$ are the polar coordinates measured from the crack tip, one can rewrite the function $\phi$ as:

$$\phi_{I,II,III}(H,z)=\frac{K_{I,II,III}}{\sqrt{2\pi(2-H)l_0}}\left(\frac{l_0}{r}\right)^{\frac{3-2H}{2}}\left\{\cos\left[\frac{(3-2H)}{2}\theta\right]-i\,\mathrm{sen}\left[\frac{(3-2H)}{2}\theta\right]\right\} \tag{21}$$

where $\phi_{I,II,III}(z)$ and $\phi'_{I,II,III}(z)=\frac{d\phi_{I,II,III}}{dz}$ are the Westergaard stress functions, which are holomorphic, i.e., analytical, and satisfy the Cauchy-Riemann conditions.

### 3.1. Calculation of the stress field with fractal roughness

*3.1.1. Solution of stress fields and displacement around the tip of a fractal crack in Mode I* $\left(G_{IC}\rightarrow K_{IC}\right)$

In *Mode I,* one has a two-dimensional tensile stress at infinity $\partial N$:

$$\Phi(r,\theta,H)=\mathrm{Re}\,\bar{\bar{\phi}}_I(r,\theta,H)+y\,\mathrm{Im}\,\bar{\phi}_I(r,\theta,H) \tag{22}$$

Note that we have applied a constant load stress in the $x$-direction in the infinite, which has no corresponding forces. This particular tensile stress is introduced to simplify the boundary condition at infinity for a uniform stress state, $\sigma_\infty$An additional stress, $\sigma_\infty$ produced in the $x$-direction by this particular tensile stress. This stress is constant because it acts on the crack plane and is therefore not affected by the internal boundary conditions that would otherwise be imposed on the surfaces of the crack. This extraneous stress can later be subtracted from the solution, if desired [32].

Analogous to what Westergaard discussed regarding various Mode I crack problems, these problems involving fractal roughness can be solved as follows:

$$\Phi(r,\theta,H)=\mathrm{Re}\,\bar{\bar{\phi}}_I(r,\theta,H)+y\,\mathrm{Im}\,\bar{\phi}_I(r,\theta,H) \tag{23}$$

where $y=r\sin\left[\frac{(3-2H)}{2}\theta\right]$, $\bar{\phi}_I(z)=\frac{d\bar{\bar{\phi}}_I}{dz}$, $\phi_I(z)=\frac{d\bar{\phi}_I}{dz}$, and $\phi'_I(z)=\frac{d\phi_I}{dz}$ are the Westergaard stress functions, which are holomorphic or analytic and satisfy the Cauchy-Riemmann conditions.

If the elastic problem can be arranged so that the crack of interest extends over a line segment of the $x$ axis ($y=0$) according to Westergaard (1939), the stresses and displacements can be obtained from the stress function $\phi(z)$ as

http://dx.doi.org/10.5772/64998

$$\begin{aligned}\sigma_{xx} &= \mathrm{Re}\,\phi_I(z) - y\,\mathrm{Im}\,\phi_I'(z) + 2A \\ \sigma_{yy} &= \mathrm{Re}\,\phi_I(z) + y\,\mathrm{Im}\,\phi_I'(z) \\ \tau_{xy} &= -y\,\mathrm{Re}\,\phi_I'(z)\end{aligned} \tag{24}$$

Note that this particular Westergaard formulation is restricted to solutions that have the properties of $\sigma_x = \sigma_y$ and $\tau_{xy} = 0$ along the $x$-axis ($y = 0$). Therefore, the biaxial stress boundary condition at infinity $\sigma_x = \sigma_y = \sigma_\infty$ is needed in order to apply the technique to the Westergaard Mode I problem.

In addition,

$$\begin{aligned}4Gu &= (k-1)\,\mathrm{Re}\,\bar{\phi} + 2y\,\mathrm{Im}\,\phi \\ 4Gu &= (k+1)\,\mathrm{Im}\,\bar{\phi} - 2y\,\mathrm{Re}\,\phi\end{aligned} \tag{25}$$

where Re and Im denote the real and imaginary parts of a complex function, and the parameter $k$ is defined individually for plane stress and plane strain by:

$$k = \begin{cases}(3-v)/(1+v) & \textit{tensão plana} \\ 3-4v & \textit{deformação plana}\end{cases} \tag{26}$$

The term $\frac{k+1}{4G}$ which appears in COD calculations can be simplified to $2/E'$ where $E' = E/(1-v^2)$ corresponds to plane strain and $E' = E$ to plane stress, and also

$$\mu = \frac{E}{2(1+v)} \tag{27}$$

This term was used to relate $\mu$ with $E$.

These quantities, in turn, can be substituted in Eq. (24), resulting in the asymptotic solution associated to the stresses, which is valid for both plane stress and plane strain in Mode I loading. By applying equations in (24), one has:

$$\sigma_{xx} = \frac{K_I}{\sqrt{2(2-H)\pi l_0}}\left(\frac{l_0}{r}\right)^{\frac{3-2H}{2}} \cos\left[\frac{(3-2H)}{2}\theta\right]\left[1-\sin\left[\frac{(3-2H)}{2}\theta\right]\sin\left[\frac{(5-2H)}{2}\theta\right]\right] \tag{28}$$

$$\sigma_{yy} = \frac{K_I}{\sqrt{2(2-H)\pi l_0}}\left(\frac{l_0}{r}\right)^{\frac{3-2H}{2}} \cos\left[\frac{(3-2H)}{2}\theta\right]\left[1+\sin\left[\frac{(3-2H)}{2}\theta\right]\sin\left[\frac{(5-2H)}{2}\theta\right]\right] \tag{29}$$

$$\tau_{xy} = \frac{K_I}{\sqrt{2(2-H)\pi l_0}}\left(\frac{l_0}{r}\right)^{\frac{3-2H}{2}} \cos\left[\frac{(3-2H)}{2}\theta\right]\left[\text{sen}\left[\frac{(3-2H)}{2}\theta\right]\cos\left[\frac{(5-2H)}{2}\theta\right]\right] \tag{30}$$

where

$$K_I^f = \sqrt{\pi L(L_0,\theta,H)} = \frac{K_I l_0^{1-H}}{\sqrt{(2-H)}} \tag{31}$$

and

$$\sigma_{zz} = v(\sigma_{xx} + \sigma_{yy}) \tag{32}$$

Similarly, following the same procedure, in plane stress and plane strain loading conditions, the asymptotic displacements or deflections $u = u(\sigma, r, \theta, a)$ around the crack tip in Mode I are determined explicitly from equation (25), as:

$$u_x = \frac{K_I^f}{8\mu\pi}\sqrt{2\pi r}\left[(2k-1)\cos\left[\frac{(3-2H)}{2}\theta\right] - \cos\left[\frac{(5-2H)}{2}\theta\right]\right] \tag{33}$$

$$u_x = \frac{K_I^f}{8\mu\pi}\sqrt{2\pi r}\left[(2k+1)\sin\left[\frac{(3-2H)}{2}\theta\right] - \sin\left[\frac{(5-2H)}{2}\theta\right]\right] \tag{34}$$

## 4. Results and analysis of a mapping of the stress field of a rough fractal fracture

To better illustrate the results obtained by Mosolov [2–4], Yavari [14, 15], and Alves, the classical fractal and stress fields at the tip of a crack in Mode I loading were mapped in this chapter in order to compare them qualitatively with the approach of other authors.

http://dx.doi.org/10.5772/64998

### 4.1. Mapping based on analytical results of fractal fractures, varying Yavari's exponent of singularity for Mode I loading

This section describes the calculation of the stress field for Mode I loading according to the model proposed by Yavari, where

$$\alpha = \frac{2 - D_D}{2} = \frac{2H - d}{2H} \tag{35}$$

where $D_D = d/H$ for $d = 1, 2$ is the divider dimension.

Substituting the values of $H = 0.0, 0.2, 0.4, 0.5, 0.6, 0.8$ and $1.0$ for stress field:

$$\begin{aligned}
\sigma_{xx} &= \frac{K_I^f}{(2\pi r)^\alpha}\left\{\cos[\alpha\theta] - \alpha\sin\theta\cos[(\alpha+1)\theta]\right\} \\
\sigma_{yy} &= \frac{K_I^f}{(2\pi r)^\alpha}\left\{\cos(\alpha\theta) + \alpha\sin\theta\sin[(\alpha+1)\theta]\right\} \\
\tau_{xy} &= \frac{K_I^f}{(2\pi r)^\alpha}\alpha\sin\theta\cos[(\alpha+1)\theta]
\end{aligned} \tag{36}$$

where $K_I^f = l_0^{(H-1)/2H}\sqrt{\pi a}$.

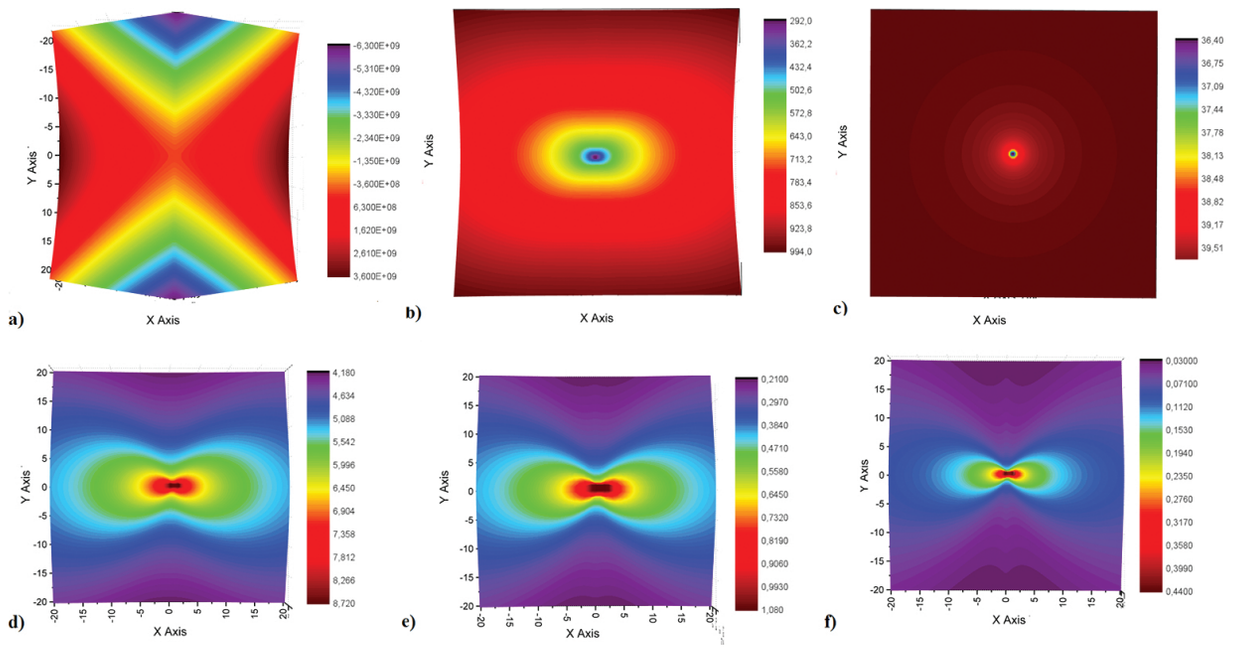


**Figure 4.** Stress field $\sigma_{xx}$ of the fractal model for Mode I fracture with singularity $1/r^\alpha$. Yavari Model $H = 0.0, 0.2, 0.4, 0.5, 0.6, 0.8$ and $1.0$.

**Figures 4**, **5**, and **6** illustrate the stress fields around a crack tip with fractal singularity degree: $\alpha$ = -1.5-0.25;0.0;0.167;0.375 and 0.5 corresponding to $H = 0.0, 0.2, 0.4, 0.5, 0.6, 0.8$ and 1.0. Note that the stress field obtained for $H = 0.0, 0.2, 0.4, 0.5$ does not show a result compatible with the reality of the stress field around of a crack tip.

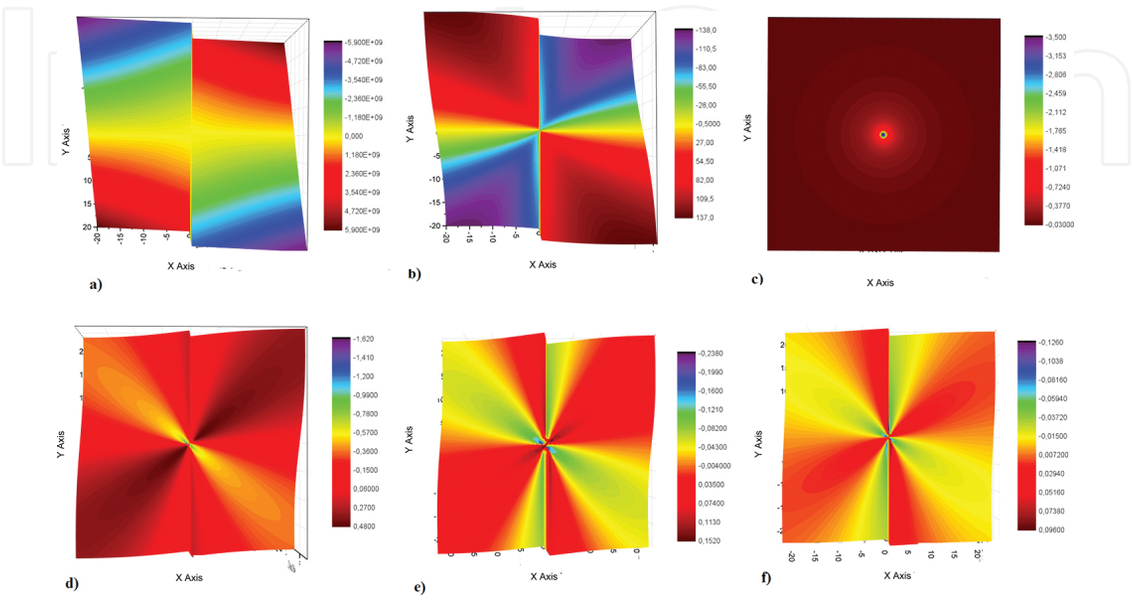


**Figure 5.** Stress field $\tau_{xy}$ of the fractal model for Mode I fracture with singularity $1/r^{\alpha}$. Alves Model $H = 0.0, 0.2, 0.4, 0.5, 0.6, 0.8$ and $1.0$.

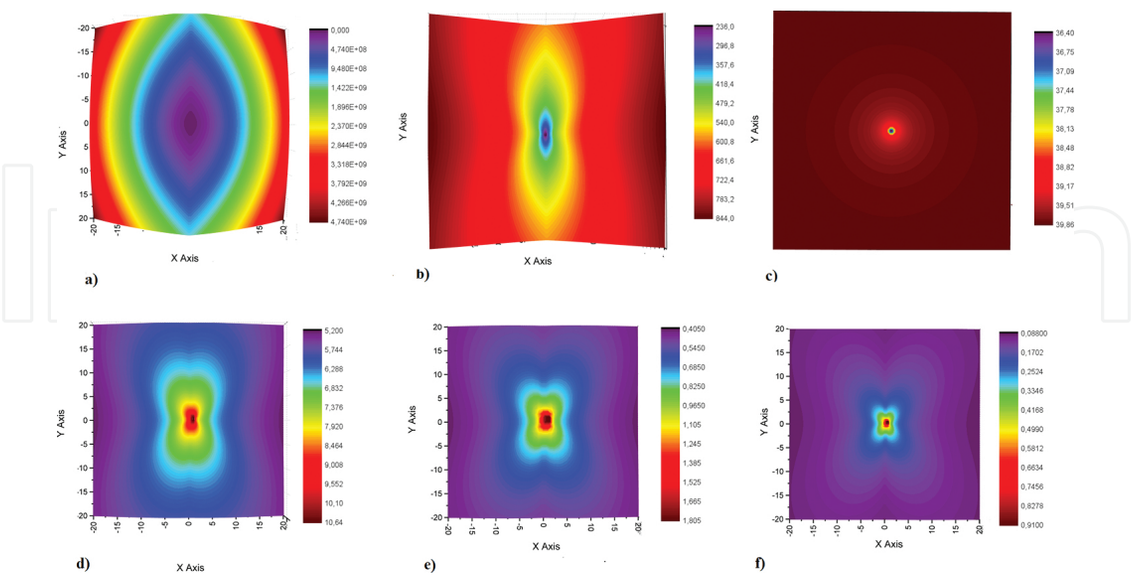


**Figure 6.** Stress field $\sigma_{yy}$ of the fractal model for Mode I fracture with singularity $1/r^{\alpha}$. Alves Model $H = 0.0, 0.2, 0.4, 0.5, 0.6, 0.8$ and $1.0$.

The idea of determining the degree of singularity of the stress field at the fractal crack tip proposed by Mosolov [2–4] and later by Yavari [14, 15] starts from the stress field expression. This, in turn, depends on the radius vector $\vec{r}$ which measures the distance from the crack tip to any point within the material. Mosolov generalizes the exponent that correlates the stress $\sigma_{ij}$ with $r$ by changing the value of the exponent given by $-1/(n+1)$ for $n$ integer to fractional exponent $-\alpha$. Balankin [13], and later Yavari [14, 15], made this generalization and found the singularity exponent based on a dimensional analysis. However, these methodologies should be further refined, since the results of the numerical simulation of the stress field around a rough crack reported by Alves et al. [19] indicate that this field is only slightly changed starting from the field around a smooth crack, obeying the Saint-Venant principle.

The calculations performed by Yavari [14, 15] are mathematically correct, but do not correspond to physical reality, in the interval for Hurst exponent of $0 \leq H \leq 0.5$, because he considered the roughness exponent as $\sim 1/H$, and hence, the singularity degree $\alpha$ can be negative, causing this singularity to disappear, as shown in the mapping for $H = 0.0$ to $H = 0.5$ in the **Figures 4**, **5**, and **6**. He considered the rough crack as a true fractal with self-affinity in the range of scale from $l_0 \leq r \leq \xi_C$ therefore, the asymptotic limits are different from a crack whose real fractality extends within a range of scales of width. It is known from experimental observation that cracks are not actually mathematical fractals and are called pre-fractals, since their self-affinity is contained within a limited range of scales: $\varepsilon_{\min} = \frac{l_0}{L_0} \leq \varepsilon \leq \varepsilon_{\max} = \frac{L_0}{L_0}$ where $l_0$ is the minimal crack length and $L_0$ is the macroscopic crack length. Thus, Alves et al. [19] propose a correction for the field around a rough crack, based on the development performed in this work.

### 4.2. Mapping based on analytical results of fractal fractures, varying Alves's exponent of singularity for Mode I loading

This section describes the calculation of the stress field for Mode I loading according to the model proposed in this chapter for

$$\alpha = \frac{3 - 2H}{2} \tag{37}$$

where $H$ is the Hurst exponent. Substituting the values of $H = 0.0,\ 0.2, 0.4, 0.5, 0.6$, and 0.8 the stress field given by (28), (29) and (30) results in the maps shown in **Figures 7**, **8**, and **9**. These figures show the stress fields around a crack tip with fractal singularity degree corresponding to $\alpha = 1.5; 1.3; 1.1; 1.0; 0.9$ and 0.7. Note that the results of the stress field obtained for $H = 0.0, 0.2, 0.4, 0.5$ is compatible with the reality of the stress field around of a crack tip.

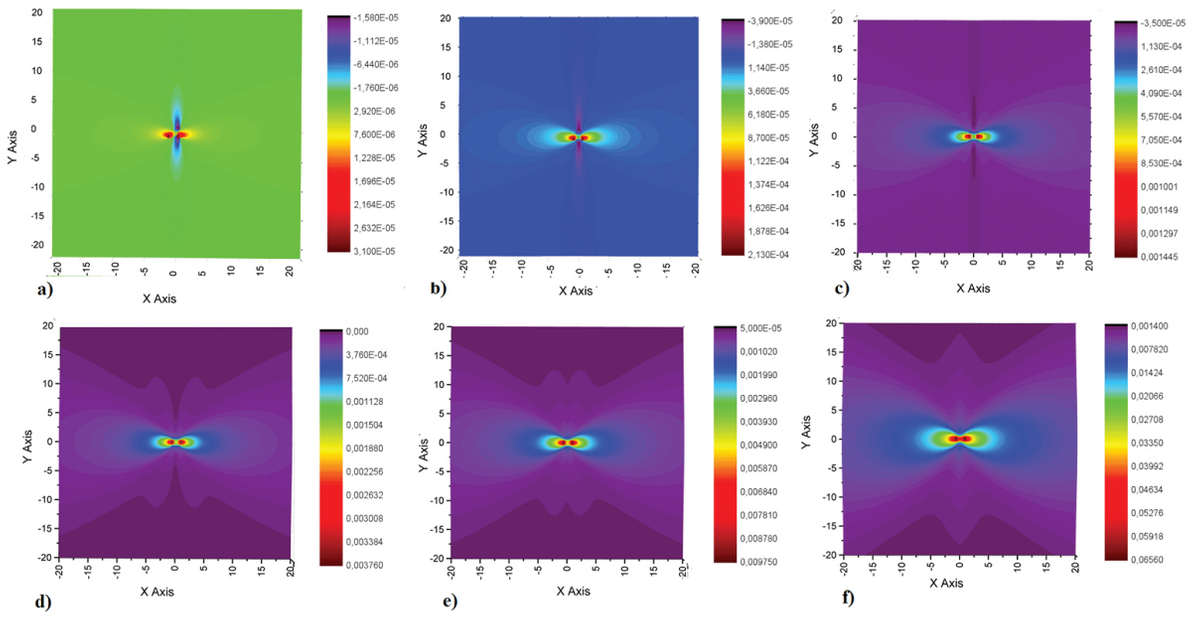


**Figure 7.** Stress field $\sigma_{xx}$ of the fractal model for Mode I fracture with singularity $1/r^{\alpha}$. Alves model for $l_0 = 0.0001$, $H = 0.0, 0.2, 0.4, 0.5, 0.6$ and $0.8$.

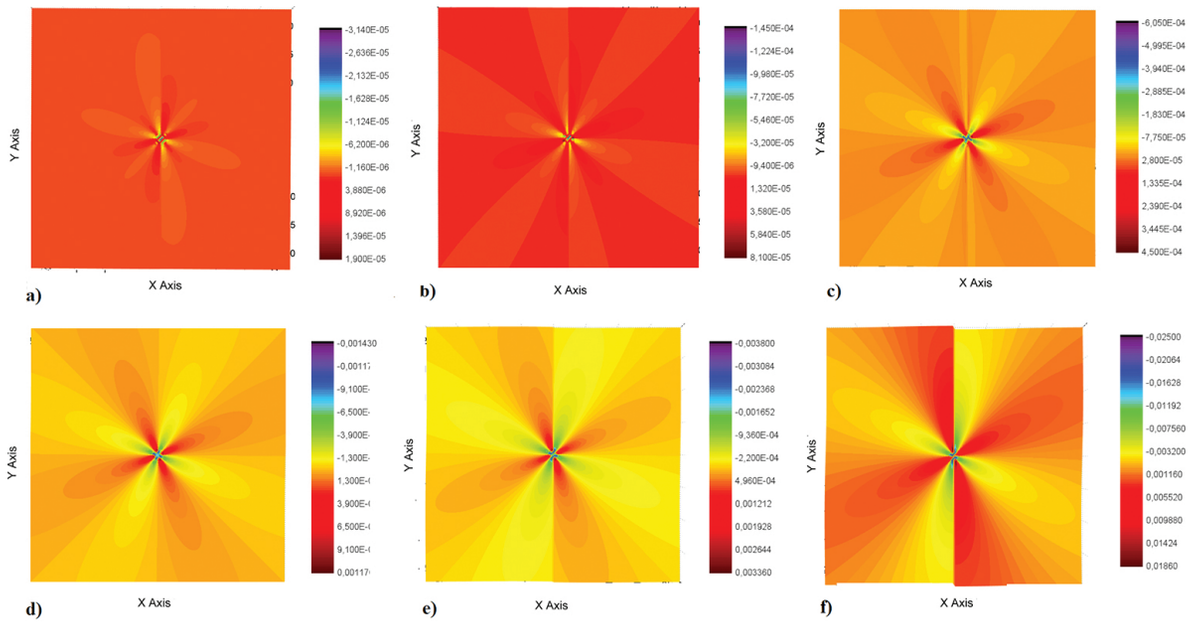


**Figure 8.** Stress field $\tau_{xy}$ of the fractal model for Mode I fracture with singularity $1/r^{\alpha}$. Alves model for $l_0 = 0.0001$, $H = 0.0, 0.2, 0.4, 0.5, 0.6$ and $0.8$.

http://dx.doi.org/10.5772/64998

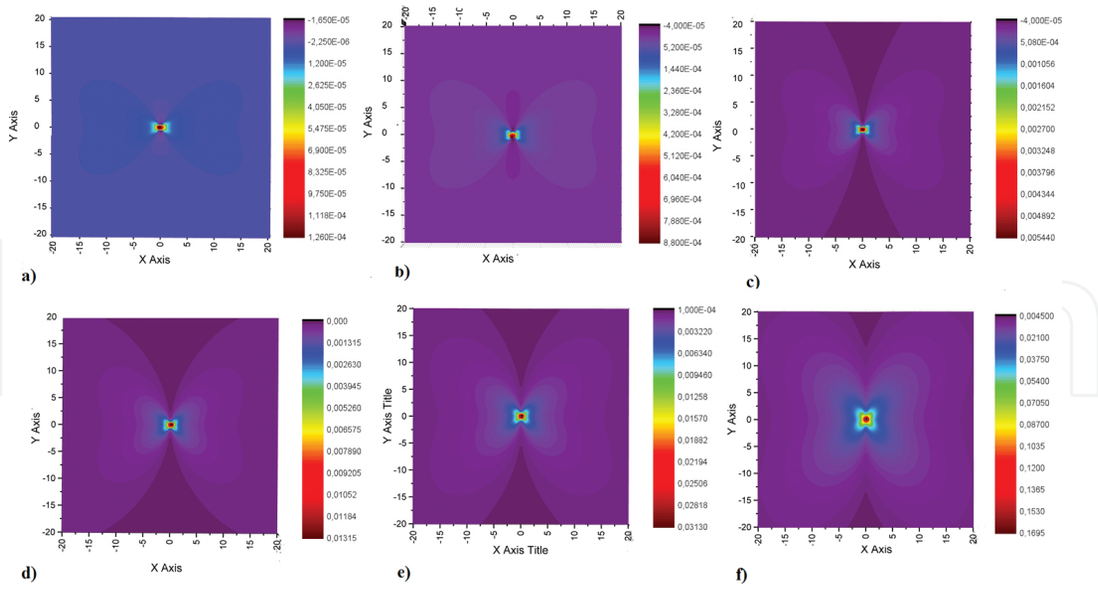


**Figure 9.** Stress field $\sigma_{yy}$ of the fractal model for Mode I fracture with singularity $1/r^{\alpha}$. Alves model for $l_0 = 0.0001$, $H = 0.0, 0.2, 0.4, 0.5, 0.6$ and $0.8$.

The stress field for $H = 1.0$ is not shown in **Figures 7**, **8**, and **9** because, in all the models presented here, the value of $\alpha = 0.5$ corresponds to the classical Euclidean field.

## 5. Discussions

A comparison of the fractal model proposed by Alves et al. [23] and the model proposed by Mosolov-Borodich [2–4, 7, 8] and Yavari [14, 15], published in the literature, leads to the following conclusions about these three theories.

In the Mosolov-Borodich model [2–4, 7, 8], cracks are treated as true mathematical fractals that extend within an infinite range of scales: $1/\infty \leq \varepsilon \leq \infty$. However, it is known from observation of nature that cracks are not actually mathematical fractals and are called pre-fractals, since their self-affinity extends only within a range of scales: $\varepsilon_{\min} = l_0/L_0 \leq \varepsilon \leq \varepsilon_{\max} = L_0/L_0$. In the fractal model proposed by Alves et al. [23], a crack is considered a pre-fractal. In considering the fractal in the model proposed by Mosolov-Borodich [2–4, 7, 8] and Yavari [14, 15], they used the coordinated function of the crack, which is a non-differentiable curve (or using Lebesgue derivative and integral, in this case). On the other hand, the fractal model proposed by Alves et al. [23], considers a pre-fractal, with a real length function of a real crack $L = f(L_0)$ which is a differentiable function, since it does not use the coordinated function (i.e., it avoids the problem of non-differentiability, since any length function is differentiable because it results in an integral, even if the coordinate function of the points is not).

In the model of Yavari a non-root square was took at the Eqs. (15), (16) and (18) until (21), whereas in the model proposed by Alves et al. [23] an exact root square was took to maintain

the symmetric dependence of the radius vector $\vec{r}$, which measures the distance from the crack tip to any point within the material.

The model of Mosolov-Borodich [2–4, 7–9], Yavari [14, 15], and Carpinteri [30, 31] at the limit of small scales, uses the renormalization theory to calculate infinitesimals in order to satisfy the Griffith criterion. Conversely, the fractal model proposed by Alves et al. [23], at the limit of small scales, uses the calculation on the $\varepsilon_{\min}$ scale to satisfy the Griffith criterion (this avoids the unnecessary complication of using a highly advanced theory). In the model of Yavari [14, 15], the rough crack length is calculated based on the assumption that $L \sim l_0^{1/H}$. The Yavari [14, 15] model divides the rough crack length into intervals $H{:}0 \leq H \leq 1/2$ (for ductile materials) and $H{:}1/2 \leq H \leq 1$(for brittle materials), while the fractal model proposed by Alves et al. [23], the model of rough crack length alternates continuously between brittle and ductile, thus satisfying what is observed in practice. In the Mosolov-Borodich [2–4, 7, 8] and Yavari [14, 15] model, the *J-R* curve is only locally independent of the path, because the integration of its radius depends on the form $r^{-D}$, Conversely, in the fractal model proposed by Alves et al. [23], the *J-R* curve is totally independent of the path because its integration does not depend on either the radius $r$ or the rough crack length, but on the roughness $\xi \equiv dL/dL_0$, which is outside of the J-integral. In the other aspects of the fractal fracture theory, the models agree with each other.

### 5.1. Influence of the local roughness of a fracture surface on the stress field at the crack tip

The graph in **Figure 10** was created by comparing the values of the Hurst exponent for the models proposed here by Alves with those of the Yavari model [14, 15]. This graph clearly shows a discontinuity in the value of the singularity of the field $1/r^{\alpha} = 1/2$. Considering that the Alves model is valid for brittle materials and the Yavari model [14, 15] is valid for ductile

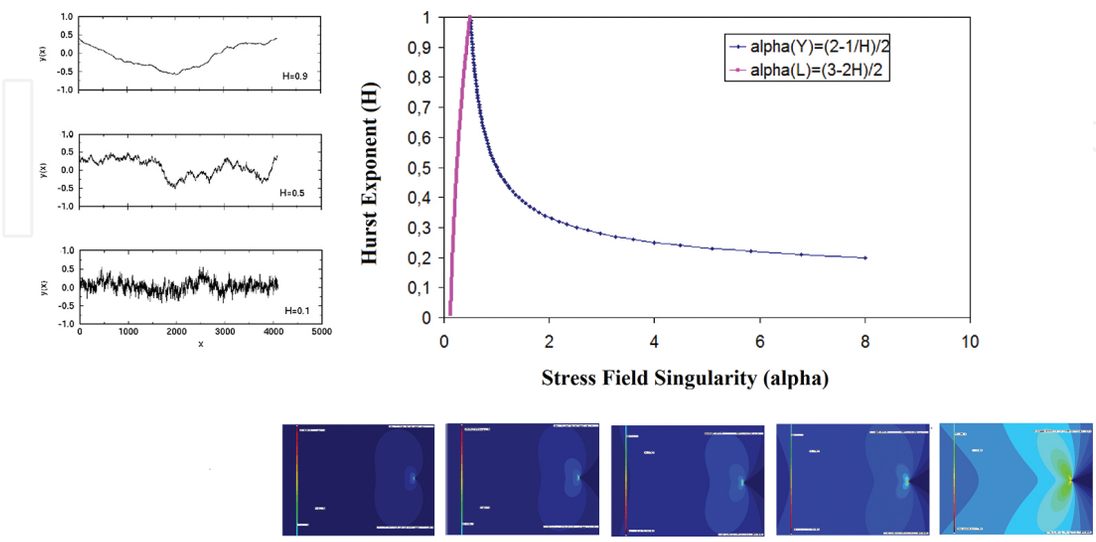


**Figure 10.** Plot of the Hurst exponent as a function of stress field singularity, calculated based on the brittle fracture predicted by Alves and on the ductile fracture predicted by Yavari.

http://dx.doi.org/10.5772/64998

materials, the point $1/r^{\alpha} = 1/2$ on the horizontal axis corresponds to the threshold of brittle-to-ductile transition, which divides the graph in **Figure 10** into two distinct regions.

When a ductile material undergoes stresses before fracturing, it produces defects that interact with pre-existing defects, causing it to become brittle before it fractures. If the material is subjected to a high loading rate it can harden even further, creating more defects and producing a higher level of stress than it displayed its initial stage. This strain hardening, which is the result of the pile-up and interaction of these defects, mainly dislocations, undoubtedly changes the degree of singularity, $1/r^{\alpha}$, of the stress field due to the change in the degree of homogeneity (exponent $\alpha$) of energy per unit volume at the crack tip. In a region at the crack tip that has been subjected to sudden loading, an increase in the degree of singularity, $1/r^{\alpha}$, of the stress field produces a fracture with some roughness, depending on the loading rate. Therefore, these effects may generate differences in the surface roughness of the newly formed crack. In other words, as the loading rate increases, the stress level at the crack tip increases because of the increase in the degree of singularity $1/r^{\alpha}$ thus increasing the tendency of the ductile material to generate an increasingly less rough crack ($H \to 1$).

On the other hand, a brittle material does not undergo strain hardening before it breaks. The material breaks upon reaching ultimate failure. In this case, roughness is simply an effect of the interaction between the crack and the microstructure of the material, where the crack may be intergranular, transgranular or mixed, depending on the material's internal mechanical strength relative to the energy imposed by the load as the crack propagates. However, if the loading rate on a brittle material is increased, roughness may increase due to the nonlinear effect of the interaction of the stress field on the microstructure of the material. In this case, cracks may appear rougher ($H \to 0$) in response to the increase in loading rate, and the loading level increases due to the increase in the degree of singularity $1/r^{\alpha}$. Therefore, **Figure 10** can therefore explain the behavior of the degree of singularity of the field, $1/r^{\alpha}$, around a crack as a function of its roughness, based on the surface roughness exponent, $\alpha$ of the fracture that propagates under different loading conditions or according to different types of materials. In **Figure 10**, the horizontal axis represents the level of singularity $1/r^{\alpha}$ and the vertical axis represents the degree of roughness, given by the Hurst exponent $H$. At $H \to 0$, namely $0 \leq H < 1/2$, the crack is rougher (hackle), while at $H \to 1$, namely $1/2 \leq H \leq 1$, the crack is smoother (mirror). In the region of $H = 1/2$, there is a mixed zone.

In a more ductile material, as the stress level increases in response to the emergence of defects in the crack tip, i.e., as the material hardens, this stress level increases due to the increase in the degree of singularity $1/r^{\alpha}$, with a rapid growth of exponent $H$. This means that, a ductile materials become embrittled, they produce an increasingly less rough crack ($H \to 1$) until they reach the threshold given by the peak of the curve. After reaching this threshold, the behavior is reversed. In other words, most brittle materials, which require a higher stress level to fracture compared to ductile materials, show a tendency to produce an increasingly rough crack ($H \to 0$) in response to increasing stress levels at the crack tip. This means that

the degree of singularity $1/r^{\alpha}$ of these materials increases in response to an increase in the loading rate. Hence, as can be seen in **Figure 10**, the threshold of ductile-to-brittle transition is at its peak when $H = 1$. The left side of this figure shows a fracture response in the form of crack roughness in a ductile material, while the right side shows a fracture response in the form of crack roughness in a brittle material.

## 6. Conclusions

The proposed model describes the stress field around a crack tip for brittle materials.

The model proposed by Mosolov-Balankin-Yavari is insufficient to portray field intensity variations around the crack tip due to roughness in the interval for Hurst exponent of $0 \leq H \leq 0.5$.

The analysis of stress field fractal models based on the coefficient of geometric instability, $\beta_L(r, \theta, H)$, proved feasible for the definition of a more realistic fractal model.

In the model presented here, the exponent $\alpha$ proposed by Mosolov is given by: $\alpha = (3 - 2H)/2$ In the model proposed by Mosolov-Balankin-Yavari, the analysis of the coefficient of geometric instability, $\beta_L(r, \theta, H)$ with variation of the Hurst coefficient, $(0 \leq H \leq 1)$ , did not present a realistic range of roughness.

The fractal behavior of the stress field can be characterized as a fractal within a finite range of scales ($\varepsilon_{\min} = \frac{l_0}{L_0} \leq \varepsilon \leq \varepsilon_{\max} = \frac{L_0}{L_0}$).

The asymptotic limit for the singularity of the stress field can lead to other results if the range of scales is not considered.

The model can provide a narrower reliability limit for the fracture stress of the brittle materials.

## Author details

Lucas Máximo Alves[1*], Marcio Ferreira Hupalo[1], Selauco Vurobi Júnior[1] and Luiz Alkimin de Lacerda[2*]

*Address all correspondence to: lucasmaximoalves@gmail.com and alkimin@lactec.org.br

1 Department of Materials Engineering, State University of Ponta Grossa – UEPG, Sector of Agricultural Sciences and Technologies, Ponta Grossa City, Paraná State, Brazil

2 LACTEC – Instituto de Tecnologia para o Desenvolvimento, DPEC/DVPE - Divisão de Pesquisas em Estruturas Civis, Centro Politécnico da Universidade Federal do Paraná, Curitiba, PR, Brazil

## References

[1] Hutchinson, J.W., Plastic stress and strain fields at a crack tip. J. Mech. Phys. Solids, 16, 337–347, 1968.

[2] Mosolov, A.B., Fractal Griffith crack, Zh. Tekh. Fiz., 61(7), 1991.

[3] Mosolov, A.B., Sov. Phys. Tech. Phys., 36, 75, 1991.

[4] Mosolov, A.B., Mechanics of fractal cracks in brittle solids, Europhys. Lett., 24(8), 673–678, 1993.

[5] Gol'dshtĕin, R.V., Mosolov, A.B., Cracks with fractal surface, Sov. Phys. Dokl., 36, 603–605, 1991.

[6] Gol'dshtĕin, R.V., Mosolov, A.B., Fractal Cracks, J. Appl. Math. Mech., 56, 563–571, 1992.

[7] Mosolov, A.B., Borodich, F.M., Fractal fracture of brittle bodies during compression, Sovol. Phys. Dokl., 37(5), 263–265, 1992.

[8] Borodich, F.M., Some fractals models of fracture, J. Mech. Phys. Solids, 45(2), 239–259,1997.

[9] Besicovitch, A.S., Sets of fractional dimensions (IV): on rational approximation to real numbers. Classics on fractals. In: Edgar, G.A. (ed) Boston, Addison-Wesley Reading, 161–168, 1993b.

[10] Besicovitch, A.S., Ursell, H.D. Sets of fractional dimensions (V): on dimensional numbers of some continuous curves. Classics on fractals. In: Edgar, G.A. (ed) Boston, Addison-Wesley Reading, 171–179, 1993c.

[11] Cherepanov, G.P., Alexander S. Balankin, Vera S. Ivanova. Fractal fracture mechanics —a review. Eng. Fract. Mech., 51(6), 997–1033, 1995.

[12] Balankin, A.S., Tamayo, P., Fractal Solid Mechanics, Revista Mexicana de Física 40,(4), 506–532, 1994.

[13] Balankin, Alexander, S., Eng. Fract. Mech., 57(2/3), 135–203, 1997.

[14] Yavari, A., The fourth mode of fracture in fractal fracture mechanics, Int. J. Fract., 101, 365–384, 2000.

[15] Yavari, A., The mechanics of self-similar and self-afine fractal cracks, Int. J. Fract., 114, 1–27, 2002.

[16] Yavari, A., Generalization of Barenblatt's cohesive fracture theory for fractal cracks, Fractals, World Scientific Publishing Company, 10(2), 189–198, 2002.

[17] Pugno, N., Ruoff, R., Quantized fracture mechanics. Philos. Mag., 84, 2829–2845, 2004.

[18] Alves, L.M., Fractal geometry concerned with stable and dynamic fracture mechanics. J. Theor. Appl. Fract. Mech. J., 44 (1), 44–57, 2005.

[19] Alves, L.M., Modelagem e Simulação do Campo Contínuo com Irregularidades: Aplicações em Mecânica da Fratura com Rugosidade, Tese de Doutorado, PPGMNE-CESEC-UFPR-Curitiba-Paraná, 2011.

[20] Alves, L.M., Foundations of measurement fractal theory for the fracture mechanics. In: Applied Fracture Mechanics, Belov, A. (ed) Intech – Open, ISBN 978-953-51-0897-9, Published: December 12, 2012 doi:10.5772/51813.

[21] Alves, L.M. et al, Analytical fractal model for rugged fracture surface of brittle materials, Eng. Fract. Mech., 232–255, 2016, doi:10.1016/j.engfracmech.2016.05.015, http://www.sciencedirect.com/science/article/pii/S0013794416302375.

[22] Alves, L.M., da Silva, R.V., Mokross, B.J., The influence of the crack fractal geometry on the elastic plastic fracture mechanics. Phys. A Stat. Mech. Appl., 295(1/2), 144–148, 2001.

[23] Alves, L.M., da Silva, R.V., de Lacerda, L.A., Fractal modeling of the *J-R* curve and the influence of the rugged crack growth on the stable elastic plastic fracture mechanics, Eng. Fract. Mech., 77, 2451–2466, 2010.

[24] Alves, L.M., de Lacerda, L.A., Fractal fracture mechanics applied to materials engineering In: Belov, A. (ed) Applied fracture mechanics, Intech-Open, doi:10.5772/52511.

[25] Alves, L.M., de Lacerda, L.A., Souza, L.A. et al., Modelo Termodinâmico para uma Linha Rugosa, apresentação de seminário na Semana da Pós-Graduação em Métodos Numéricos em Engenharia, Universidade Estadual de Ponta Grossa,·2010, doi: 10.13140/RG.2.1.4309.4881.

[26] Ohr, S.M., Narayan, J., Electron microscope observation of shear cracks in stainless steel single crystals. Phil. Mag. A., 41, 81–89, 1980.

[27] Xin, G., Hangong, W., Xingwu, K., Liangzhou, J., Analytic solutions to crack tip plastic zone under various loading conditions. Eur. J. Mech. A/Solids. 29, 738–745, 2010.

[28] Westergaard, H., Bearing pressures and cracks. J. Appl. Mech. A, 49–53, 1939.

[29] Irwin, G.R., Fracture dynamics, Fracturing of metals. Cleveland, American Society for Metals, 147–166, 1948.

[30] Carpinteri, A, Chiaia, B., Cornetti, P., A fractal theory for the mechanics of elastic materials, Mater. Sci. Eng., A365, 235–240, 2004.

[31] Carpinteri, A., Puzzi, S., Complexity: a new paradigm for fracture mechanics, Frattura Ed Integrità Strutturale, 10, 3–11, 2009, doi:10.3221/Igf-Esis.1001.

[32] Unger, David J. "Analytical Fracture Mechanics", Academic Press, ISBN 0-12709120-3, 1995.